Journal of the European Ceramic Society **15** (1995) 777–785

0955-2219/95/$9.50

0955-2219(95)00048-0

The Interrupted Static Fatigue Test for Evaluating Threshold Stress Intensity Factor in Ceramic Materials: A Numerical Analysis

Vincenzo M. Sglavo & David J. Green

Department of Materials Science and Engineering, The Pennsylvania State University, University Park, PA 16802, USA

(Received 1 August 1994; revised version received 7 February 1995; accepted 14 February 1995)

Abstract

The interrupted static fatigue (ISF) test can be used to evaluate the threshold for sub-critical crack growth, K_{th}. A critical theoretical analysis of this technique is presented in order to elucidate its advantages and limitations and to furnish some suggestions for a more definitive procedure for evaluating K_{th}. It was concluded that a critical parameter in the ISF procedure is the duration of the static hold time. In particular, one should demonstrate that the calculated value of K_{th} does not change when this holding time is increased. Moreover, the applied stress must be chosen such that a significant fraction of samples fail in the hold period. Two different approaches are suggested for calculating the value of K_{th} from experimental data. The first approach is considered preferable for materials with larger Weibull moduli and the threshold is determined from the applied stress intensity factor at which 50% of samples fails during the stress hold. In the second approach, the stress intensity factor applied to the weakest specimen during the stress hold is calculated for various hold times. Once this value becomes independent of hold time, it is equivalent to the threshold.

1 Introduction

The use of glasses and ceramic materials in structural applications can be limited by the phenomenon known as sub-critical crack growth. For ceramics that exhibit this fatigue behaviour, strength becomes dependent upon time and environmental conditions. The design of structural components consisting of materials that exhibit fatigue behaviour must proceed by the estimation of a design stress, which corresponds to a required minimum failure time.

Some studies on sub-critical crack growth in glasses and ceramics have shown that this phenomenon seems to have a lower limit in the sense that crack propagation velocities tend to zero for some particular value of the applied stress intensity factor, K_{th}. This is termed the fatigue limit or the threshold stress intensity factor.[1–15] From an engineering design point of view, the existence of a fatigue limit turns out to be extremely desirable, as it allows an applied stress to be defined, below which delayed failure does not occur.

In spite of the importance of the fatigue threshold, no comprehensive test methodology has been presented for its determination. In early works on sub-critical crack growth in glasses and ceramics, specimens, usually pre-cracked, were loaded at different stress levels and the lifetime was determined.[1–7,9] The 'endurance limit' was defined as the stress at which the fatigue curve shows an asymptotic limit. For glass in a moist environment, values ranging from 0·2 to 0·4 times the strength measured in liquid nitrogen were obtained.[5] The same approach has also been used in more recent works.[16–18]

Studies devoted to sub-critical crack velocity determination as a function of the applied stress intensity factor showed, in some cases, the existence of a threshold below which crack motion did not occur. In these cases, fracture mechanics specimens such as the double cantilever beam (DCB) and double torsion geometries were used and crack advancement was measured as a function of time.[8,10,13,14,19–21]

The difficulty with the methodologies described above is that extremely long experimental times are necessary to evaluate the crack growth at these low stress levels. In fact, the fatigue limit is usually extrapolated from stress or stress intensity factor data to obtain information at long times.

The difficulties, outlined above, can be by-passed by using some indirect methods. For example, in the work of Michalske, DCB glass specimens were loaded in water at a stress intensity factor value of

0·225 MPa √m and aged in this state for fixed periods.[22] The stress intensity factor was then raised and crack motion as a function of time was recorded. The existence of a stress corrosion limit in glass, postulated to be the result of crack tip blunting, was exhibited by observing a delay in the crack growth upon reloading. A fatigue limit $<0{\cdot}25$ MPa √m in soda lime silicate glass was proposed.[22]

An approach that is experimentally easier was presented by Dutton and Rogowski[23] and Wilkins and Dutton.[24] In their studies, alumina and glass samples were loaded in a 'corrosive' environment and the load was maintained for times of the order of a few hours. The strength was then measured and compared to the initial strength. This has been termed the interrupted static fatigue (ISF) test. The same technique has been used by Hayashi *et al.* to measure the fatigue limit of borosilicate glass rods in water.[25]

Tressler and coworkers[26–29] have further developed the approach proposed by Dutton and Rogowski.[23] In studies on silicon carbide and silicon nitride ceramics at high temperatures, they measured the average strength of samples aged under different loads. The threshold stress intensity factor was calculated from the stress level above which samples failed during the static hold part of the test. Nevertheless, the lack of a solid theoretical background sometimes made the interpretation of the data difficult.[26–29] Tanaka and Pezzotti pointed out that some of the data proposed by Tressler and coworkers do not represent the real fatigue limit but are the result of a typical time-to-failure test.[30]

In the following study, a theoretical analysis on the interrupted static fatigue test is presented. The behaviour of silicon carbide at high temperatures and of glass in water is simulated using fracture mechanics so that the conditions for the correct evaluation of the fatigue limit can be highlighted. The results of the theoretical analysis allow some suggestions regarding the methodology for threshold stress intensity factor determination to be proposed.

2 Theoretical Approach

In order to describe the strength degradation that occurs in the interrupted static fatigue test, a function describing the sub-critical crack propagation velocity is required. The crack growth behaviour is usually expressed as a power function of the stress intensity factor K and can be written as follows:

$$v = \frac{dc}{dt} = v_0 \left(\frac{K}{K_c}\right)^n \quad \text{if } K > K_{th} \tag{1a}$$

$$v = 0 \quad \text{if } K < K_{th} \tag{1b}$$

where K_c corresponds to the fracture toughness, v_0 and n are constants which depend upon the material and the environment, K_{th} is the threshold for sub-critical crack growth and c is the crack length.

The stress intensity factor K, associated with a 'crack-like' flaw subjected to an applied stress σ, is given by

$$K = \sigma \Psi \sqrt{c} \tag{2}$$

where Ψ is the geometric factor that includes the effect of flaw shape, boundary interactions and loading geometry. In the absence of residual stress fields, the strength S, associated with a crack of length c, can be written as

$$S = \frac{K_c}{\Psi \sqrt{c}} \tag{3}$$

According to eqn (1a), when a constant stress, σ_h, is applied for a time t and $K > K_{th}$, the flaw size increases from the initial value c_0 to a final value c_1. Correspondingly, strength decreases from S_0 to S_1. Substitution of eqn (2), with $\sigma = \sigma_h$, into eqn (1) and subsequent integration allows one to evaluate S_1 as a function of hold time t as

$$S_1 = \left(S_0^{n-2} - \frac{\sigma_h^n t}{B}\right)^{1/(n-2)} \quad \text{if } K > K_{th} \tag{4a}$$

$$S_1 = S_0 \quad \text{if } K < K_{th} \tag{4b}$$

where

$$B = \frac{2K_c^2}{(n-2)\Psi^2 v_0} \tag{5}$$

When n is a real number, eqn (4a) is not defined for $\sigma > \sigma^* = (B\, S_0^{n-2}/t)^{1/n}$, the condition for which $S_1 = 0$.

Equation (4) can also be expressed in terms of the stress intensity factor K_h, applied at the start of the static hold. From eqns (2) and (3),

$$\sigma_h = S_0 \frac{K_h}{K_c} \tag{6}$$

and thus, for $K_h > K_{th}$, eqn (4a) becomes

$$S_1 = S_0 \left(1 - \frac{S_0^2 K_h^n t}{K_c^n B}\right)^{1/(n-2)} \tag{7}$$

In this case, S_1 is not defined for $K_h > K^* = K_c\,[B/(S_0^2 t)]^{1/n}$. The importance of this condition resides in the fact that, when a stress intensity factor larger than K^* is applied for a time t, the final strength S_1 is zero. This condition can also be defined in terms of the ratio $\kappa = K_h/K_c$, as

$$\kappa^* \left(\frac{2c_0}{(n-2)tv_0}\right)^{1/n} \tag{8}$$

3 Simulation Results

On the basis of the theoretical background developed in the previous section, the behaviour of silicon carbide at 1400°C and soda-lime silicate glass in water at room temperature was simulated. The properties used in the calculations are given in Table 1.[31,32] In these initial calculations, average strength values were used. The effect of strength variability will be explored later.

Figure 1 shows the strength of SiC after the ISF test as a function of the applied stress for three different holding times, as calculated from eqn (4), in the absence of a threshold. Sub-critical crack growth is responsible for the strength decrease that occurs over a small range of applied stress values. This behaviour demonstrates that, even in absence of a threshold for fatigue, strength remains practically constant for most of the lifetime of the sample. It can also be observed that the stress value (σ^*) at which strength 'drop-off' occurs, decreases for increasing hold time.

Diagrams such as Fig. 1 can also be given in terms of the stress intensity factor (eqn (7)), as shown in Fig. 2. In this case, the threshold for sub-critical crack growth was assumed to be 1 MPa $\sqrt{m}$.[31] A distinct strength drop-off is still evident and K^* decreases for increasing hold times until the threshold is reached. At this point, further increases in hold time do not have any influence on the stress intensity factor corresponding to the strength drop-off.

Figures 1 and 2 illustrate some important features regarding threshold measurement by the ISF test. When S_1 is measured to be equal to the initial strength S_0, it is not possible to definitely conclude that this is the effect of K being lower than the threshold. In addition, as shown in Fig. 2 for SiC at 1400°C, hold times during the ISF test must be longer than 44·2 h in order to guarantee that the strength degradation is only a result of the stress intensity factor being above the threshold.

Table 1. Properties of SiC and soda-lime glass considered in this study[31,32]

S_0 (MPa)	K_c (MPa $\sqrt{m}$)	n	B (MPa^{2}s)
470	2·7	21	14·23
130	0·75	19·3	0·19

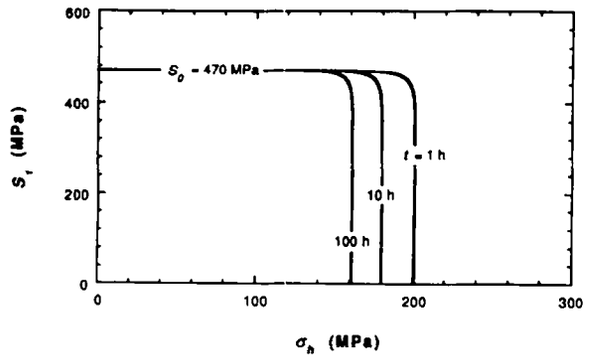

Fig. 1. Strength S_1 of SiC after the ISF test as a function of the applied stress σ_h for three different holding times.

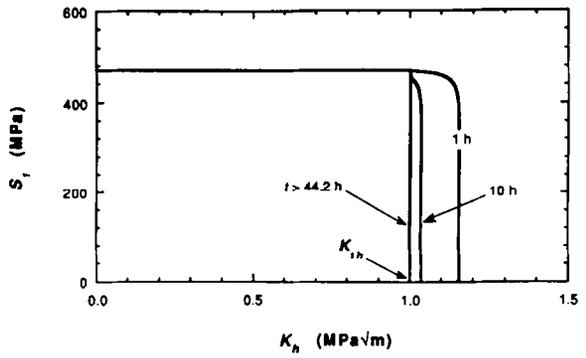

Fig. 2. Strength S_1 of SiC after the ISF test as a function of the applied stress intensity factor K_h for increasing holding times. A fatigue threshold equal to 1 MPa $\sqrt{m}$ was assumed.

The importance of the hold time on the performance of the ISF test can be highlighted further by Fig. 3, in which the stress intensity factor at which strength drop-off occurs (K^*) is plotted as a function of t. It is clear that if the material possesses a threshold, it is critical to ensure the strength loss due to sub-critical crack growth is occurring at the threshold conditions. Diagrams in Fig. 3 were calculated starting from initial strength values of 470, 149 and 47 MPa. The first of these values was that used in Table 1 while the other two were calculated by assuming that the initial crack size was 10 and 100 times larger. Such behaviour would be obtained if cracks were purposely introduced into the test specimens. The behaviour in Fig. 3 indicates that the presence of larger flaws leads to an increase in the time necessary for defining the threshold behaviour in the ISF test. Indeed, the introduction of artificial larger cracks, in order, for instance, to reduce the strength scatter, has a negative impact on the efficiency of the test methodology in terms of time management.

Calculations similar to those presented for SiC at 1400°C were also performed for soda-lime silicate glass in water at room temperature. The most

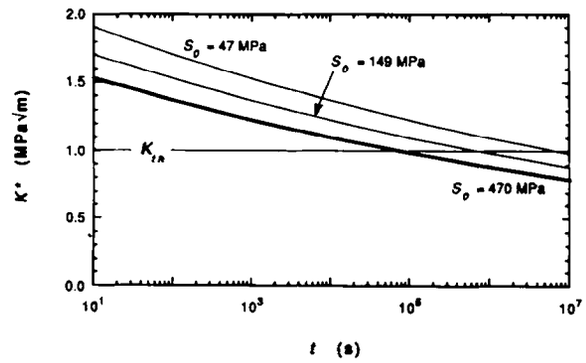

Fig. 3. 'Drop off' point K^* for SiC as a function of the holding times for different initial strengths S_0.

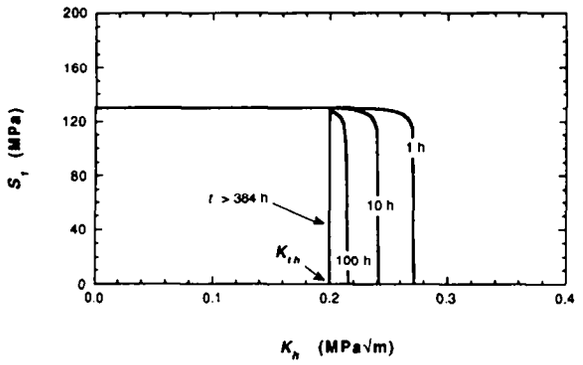

Fig. 4. Strength S_1 of soda-lime silicate glass after the ISF test as a function of the applied stress intensity factor K_h for increasing holding times. A fatigue threshold equal to 0·2 MPa √m was assumed.

significant result is shown in Fig. 4, where the strength after holding under constant stress is plotted as a function of K, for different dwell times. In this case a threshold for sub-critical crack growth was assumed to be 0·2 MPa √m.[11] For this case, hold times in excess of 384 h were found to be necessary to ensure the threshold is being measured properly for soda-lime silicate glass. Clearly, lower values of the ratio K_{th}/K_c would further increase the necessary hold times for threshold detection.

Simulation of the strength degradation behaviour of soda-lime glass was analysed further in order to point out the influence of an interrupted static fatigue test on the strength distribution. Thus far, calculations were developed by considering only the average strength (Table 1). Due to the typical large scatter shown by the strength of ceramic materials, a complete analysis should not leave out of consideration the variation in the initial crack sizes. This is an important feature as it implies a variability in K_h.

Glass strength was assumed to follow a Weibull distribution, as defined by the relationship[33]

$$F = 1 - \exp\left[-A\left(\frac{S}{\sigma_0}\right)^m\right] \tag{9}$$

where F is the failure probability, A is a constant depending on the geometry of the specimen and of the test, while σ_0 and m represent the scale parameter and the shape factor, or Weibull modulus, respectively. The constant A was assumed to be equal to 1 for easier calculation, but this does not compromise the generality of the analysis. The strength distribution was generated by assuming a mean strength S_m and a Weibull modulus equal to 130 MPa (Table 1) and 5, respectively.[33] The scale parameter σ_0 was determined by the relation[33]

$$\sigma_0 = \frac{S_m}{\Gamma(1 + 1/m)} \tag{10}$$

where Γ is the gamma function. Two situations, corresponding to a number of test specimens (N) equal to 10 and 100, respectively, were considered. Failure probability was calculated as $F = j/(N + 1)$, j being the rank in the ascending strength distribution.[33] Discrete values of the strength were obtained from eqn (9). The simulation of strength distribution variations after ISF testing was performed by considering holding times (t) ranging from 1 to 1000 h and applied stresses (σ) of 15, 30, 45 and 60 MPa. As earlier, a threshold stress intensity value of 0·2 MPa √m was assumed. Each element of the initial strength distribution S_{0j} (j = 1,N) was associated with a particular initial flaw size c_{0j}. This value was used to evaluate the stress intensity factor K_j applied to each specimen by eqn (2), once the hold stress was defined. Depending on the K_j value, the strength S_{1j} was calculated by eqn (4) as a function of hold time and applied stress.

Figure 5(a) shows the Weibull plot of the strength distributions after the holding at different stress levels for 1 h, for N = 100. The failure probability of specimens surviving the static hold were calculated as a censored distribution. The initial distribution, corresponding to an applied stress equal to 0, is obviously represented by a straight line.[33] Increased values of σ lead to significant changes in the strength distribution. This appears

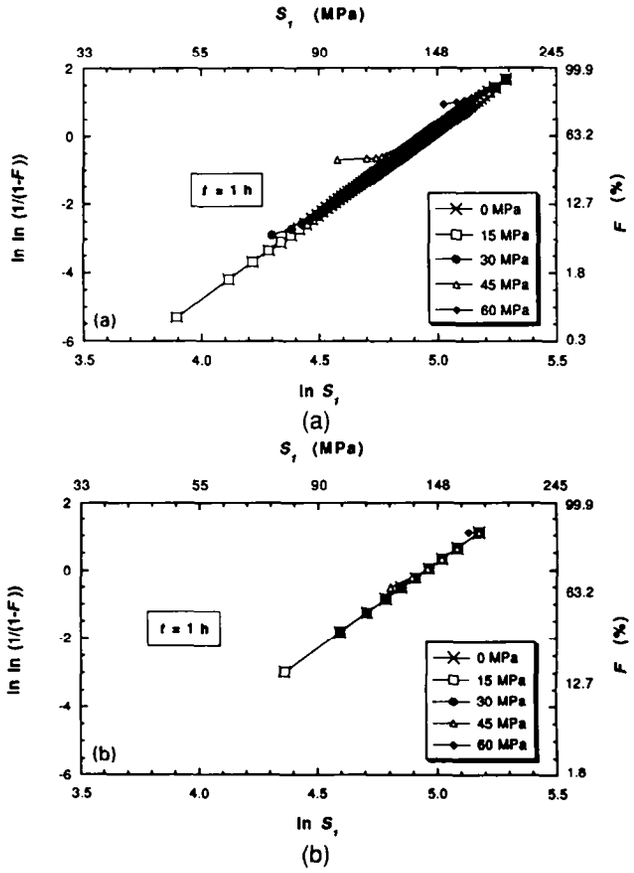

Fig. 5. Weibull plot of the strength distribution of soda-lime silicate glass after the holding at different stress levels for 1 h. The initial strength distribution corresponds to the applied stress of 0 MPa. (a) Number of specimens, N = 100, (b) N = 10.

as a 'twist' in the distribution, which is truncated for specimens that fail during the static hold. Sub-critical growth accounts for these effects. The larger the defect, the higher the stress intensity factor applied during the hold and this increases the amount of sub-critical crack growth. Thus, larger flaws can grow significantly or even fail during the constant stress period. Similar trends were also observed when $N = 10$, although the 'twisting' becomes more difficult to distinguish, as shown in Fig. 5(b). Clearly, the behaviour in a real experimental test would be further complicated by the actual scatter in the c_0 values and statistical sampling effects.

The effect of increasing hold time is shown in Fig. 6, for $N = 100$ and, as expected, a larger number of specimens fail during the stress hold for a given applied stress (all specimens fail when $\sigma = 60$ MPa and $t \geq 100$ h). A limit is reached when an increased hold time does not affect the distributions further, i.e. the twist in the distribution disappears, as shown in Fig. 6(c) and (d). This implies that all the specimens that fail in the hold had K values above the threshold, while those that survived were below the threshold. The same behaviour was also observed for $N = 10$.

Changes in strength distribution after specimens have been held at particular stress levels have been used in some previous studies as a means to identify the threshold for sub-critical growth in glass.[24,25] For example, Wilkins and Dutton[24] and Hayashi *et al.*[25] determined K_{th} for soda-lime glass at 400°C and for borosilicate glass in water at room temperature, respectively. In these studies the threshold was defined as the point in the strength distribution at which the 'twisting' starts. This approach is based on the assumption that the element of the distribution from which 'twisting' starts corresponds to the specimen subjected to a stress intensity factor equal to or lower than the threshold. If the data output used to draw Figs 5 and 6 are considered, the elements subjected to $K = K_{th}$ can easily be identified. The points corresponding to these specimens are marked with the letter X in Fig. 7, which shows three of the distributions presented in Fig. 5(a). It is evident that the points denoted as X_1 and X_2 are not the same as the points at which the twisting becomes significant. As already pointed out in the earlier analysis, specimens that do not show any strength degradation may not have been subjected to a stress intensity factor value lower than K_{th} (Fig. 1). When experimental data are considered, detection of the points denoted as 'X' in Fig. 7 is an even more formidable task as the current analysis did not include the type of scatter seen experimentally. If points like those marked with 'Y' in Fig. 7, are considered in place of 'X', this leads to an overestimation of the fatigue limit. For example, the use of points Y_1 and Y_2 leads to threshold estimates of

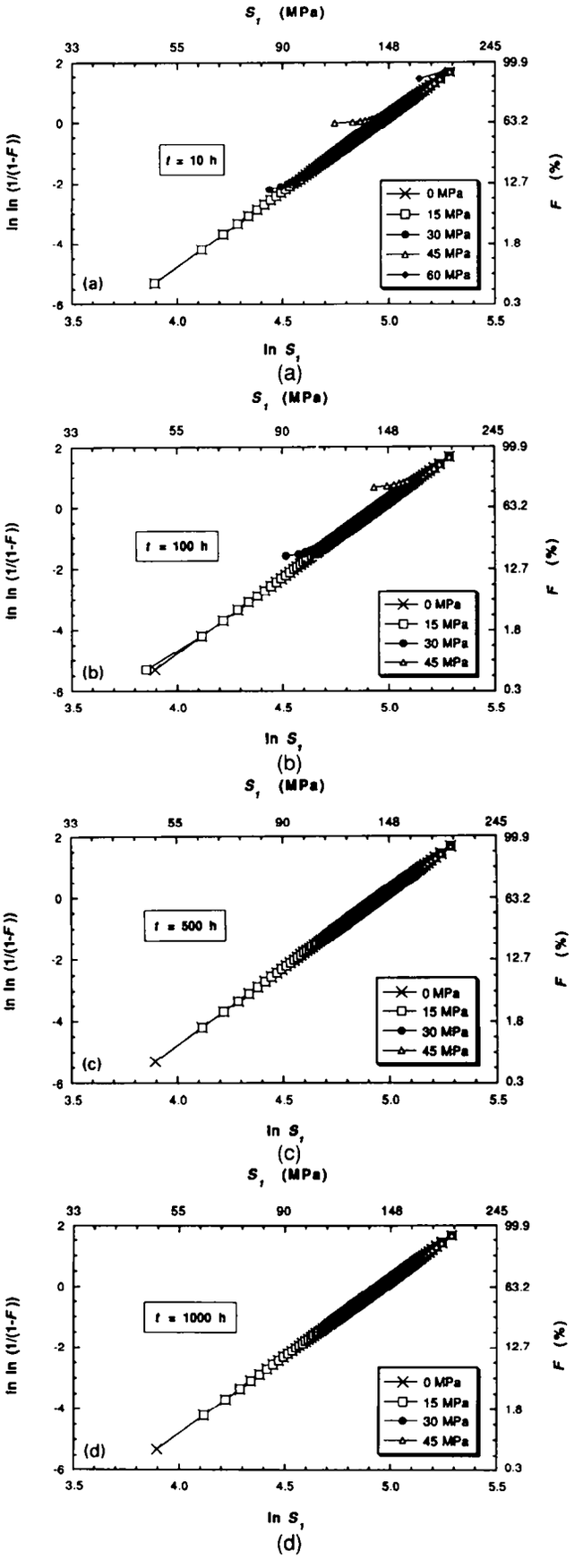

Fig. 6. Weibull plot of the strength distribution of soda-lime silicate glass after the holding at different stress levels for (a) 10 h, (b) 100 h, (c) 500 h and (d) 1000 h. The initial strength distribution corresponds to an applied stress of 0 MPa.

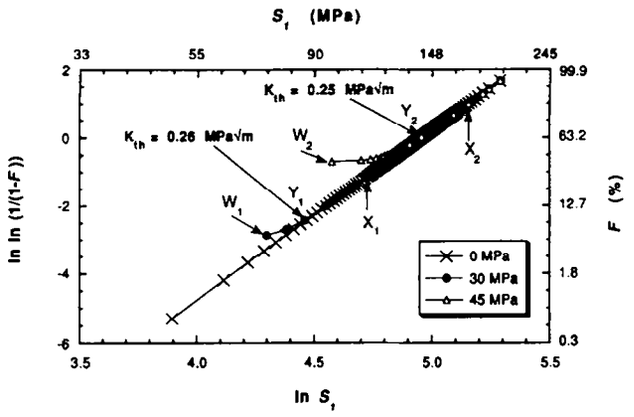

Fig. 7. Weibull plot of the strength distribution after the holding at two different stress levels for 1 h (Fig. 5(a)). The initial strength distribution corresponds to the applied stress of 0 MPa. Some elements of the distributions were removed around points marked with 'X' and 'Y' for better clarity. Explanation of points 'X', 'Y' and 'W' is given in the text.

0·26 and 0·25 MPa √m, respectively, instead of the value assumed in the analysis (0·2 MPa √m).

On the basis of the presented simulation (Figs 5 and 6), a different approach to threshold estimation is proposed. If the weakest specimen of the distribution (marked as 'W' in Fig. 7) is considered, the corresponding stress intensity factor K_W tends to, and then equals, the threshold, as the holding time is increased, as shown in Fig. 8. This shows that calculated K_W values correspond to the previously assumed fatigue limit (0·2 MPa √m) for $t \geq 500$ h, when $N = 100$. One would expect that the number of specimens used for each test condition would be important, as this increases the range of K_h values (Fig. 5); that is, one is more likely to obtain $K_h < K_{th}$ and more specimens would break during the constant stress phase. Clearly, using a larger number of specimens influences both economics and duration of the experimental work.

A final step in the simulation was performed by using data shown in Fig. 6 in order to plot the strength as a function of the applied stress intensity factor. Average values (K_{av}) of the stress intensity factor applied during the hold were calculated from the initial average strength from eqn (6). The average strength after holding, and

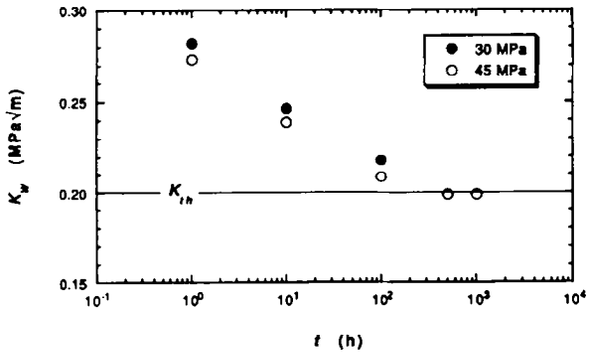

Fig. 8. Stress intensity factor K_w corresponding to the weakest sample of the strength distributions after the ISF test at stress levels of 30 and 45 MPa (Figs. 5(a) and (6)) as a function of the holding time t. Symbols at t equal to 500 and 1000 h are overlapped.

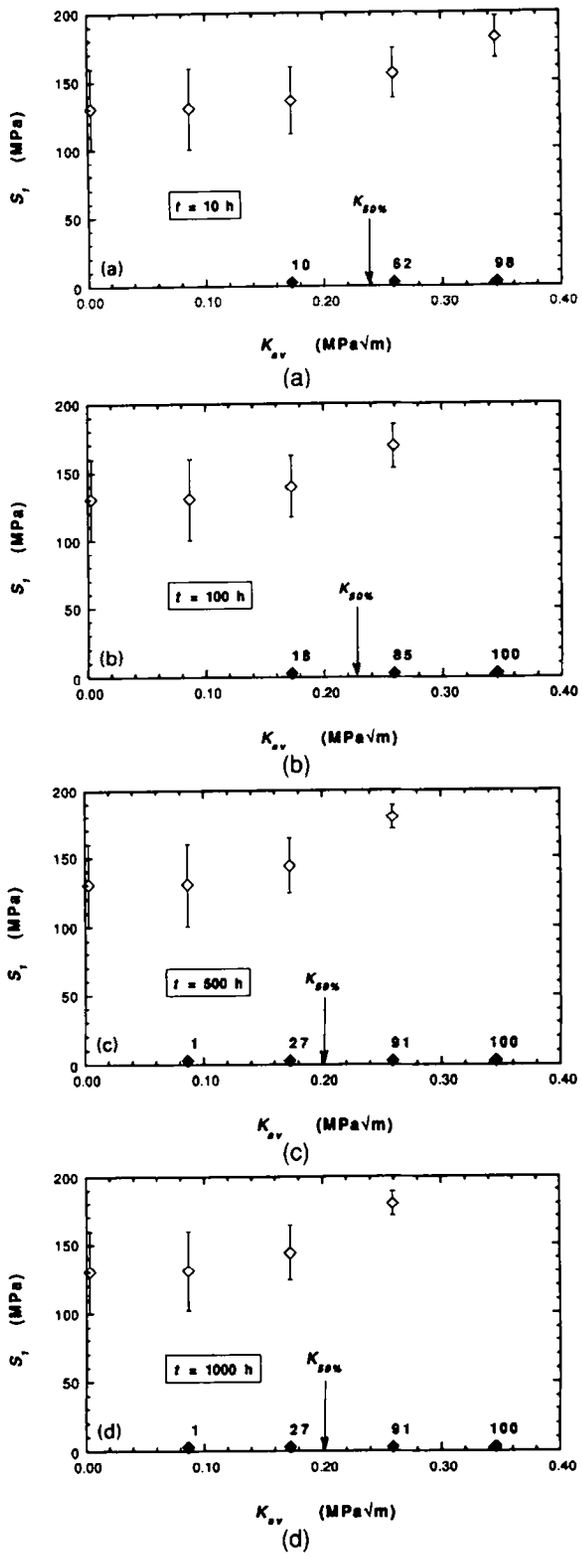

Fig. 9. Average strength S_f after the holding at different stress levels as a function of the applied stress intensity factor K_{av} for holding times of (a) 10 h, (b) 100 h, (c) 500 h and (d) 1000 h. The initial strength is shown at $K_{av} \approx 0$ MPa √m. Both S_f and K_{av} were calculated on the basis of results shown in Fig. 6. The numbers close to the solid symbols represent the number of specimens failing during the hold. The stress intensity factor $K_{50\%}$ corresponding to failure of 50% of the specimens during the hold, was calculated by linear interpolation.

corresponding standard deviation, were determined from data in Figs 5 and 6. Figure 9 shows the results for $N = 100$. The number of samples failing during the stress hold is also shown and the stress intensity factor ($K_{50\%}$) corresponding to the failure of 50% of the specimens during the hold is shown. $K_{50\%}$ is meant to represent the value of the stress intensity factor at which the average of the strength S_1 tends to zero in eqn 4(a). In Fig. 9, $K_{50\%}$ was calculated, by linear interpolation, as the stress intensity factor at which 50 specimens failed. As was previously pointed out, it is evident that $K_{50\%}$ tends to, and then equals, the fatigue limit as t increases. These calculations suggest a second approach to threshold determination, i.e. design the ISF test such that specimens break during the hold time and then increase the hold time.

4 Suggestions for a Correct Procedure for the ISF Test

The results presented in the last section suggest appropriate procedures for the measurement of the fatigue limit for sub-critical crack growth.

Two different approaches have been suggested. The first one is related to the determination of the strength distribution changes for specimens that survive the hold period, while the second one considers the changes in the average strength values. Suggested procedures for these two approaches are given below.

4.1 Strength of weakest specimen approach

The initial strength distribution (S_{0j}) must be determined in an inert environment. Samples are then subjected to the ISF test using constant stress σ for a time t. Knowledge of the fatigue parameters n and B from dynamic fatigue experiments is very useful as it allows one to estimate σ^* and K^* values from eqns (4) and (7). If an estimated value of the threshold is available, σ and t can be decided on the basis of σ and K^*, such that some failures will occur during the static hold. Strengths are also measured in the inert environment after the ISF test to obtain the distribution S_{1j}. A strength of zero is assigned to samples that fail during the stress hold and this allows one to obtain the censored distributions such as those illustrated in Figs 5 and 6. The weakest sample is identified and its rank in the strength distribution allows its strength (S_{0w}) to be defined from the previously determined initial strength distribution. The stress intensity factor K_w applied to this weakest sample can then be calculated as:

$$K_w = K_c \left(\frac{\sigma}{S_{ow}} \right) \tag{11}$$

Knowledge of the toughness K_c is essential for a precise definition of K_w. The value of K_w is then determined at the same hold stress but with increasing hold times. When K_w becomes invariant with hold time, $K_w = K_{th}$.

This first approach is considered to be preferable for materials with lower Weibull moduli. In fact, due to the large strength scatter when m is low, only a few trials are necessary to identify the stress and times required for the hold periods. Conversely, for very narrow strength distributions, several trials could be necessary before the optimal applied stress value can be identified.

It has been outlined that the strength measurement should be performed in an inert environment. Determination of K_w from eqn (11) requires the inert strength to be known. Unfortunately, inert conditions are sometimes difficult to obtain, especially when the behaviour of materials at high temperatures is considered. When the strength is measured in an active environment, it is usually lower than the inert value and this results in an overestimation of the threshold.

4.2 Hold period failure approach

In this alternative approach, the average initial strength S_{0av} is measured. Then samples are subjected to some ISF tests in which different stress levels are used for a certain time t. In this case, values of σ and t can be a decided on the basis of the assumption of a particular value for the threshold and from a knowledge of n and B. The number of samples failing during the hold at each stress level is recorded and the applied stress corresponding to 50% of samples failing during the hold ($\sigma_{50\%}$) can be calculated by easy linear interpolation. The corresponding stress intensity factor is given by

$$K_{50\%} = K_c \left(\frac{\sigma_{50\%}}{S_{0av}} \right) \tag{12}$$

As in the previous case, the hold time is increased and, once $K_{50\%}$ becomes invariant with hold time, $K_{50\%} = K_{th}$.

This second approach is considered to be appropriate for materials with large Weibull moduli. First of all, the precision of the average strength and of the number of samples failing during the hold is higher for larger values of m. In addition, several trials could be necessary to determine $\sigma_{50\%}$ precisely for wider strength distributions. Interestingly, in this approach, determination of the strength after the holding is not even necessary unless the purpose of the study is also to detect some strengthening effect taking place during the hold, for instance a strength increase could be correlated to crack tip blunting.[34–37]

5 Conclusions

A theoretical simulation of the interrupted static fatigue (ISF) tests, used for the evaluation of the fatigue threshold K_{th}, was presented. The behaviour of SiC at 1400°C and soda-lime glass in water at room temperature was analysed using fracture mechanics principles. The analysis considered changes in both the average strength values and strength distribution as a result of a period of constant stress. The duration of the ISF test and the applied stress turned out to be extremely important for a correct evaluation of the threshold. Optimal values for these two parameters can be calculated *a priori* from the fatigue parameters n and B, and from the assumption of a particular value of K_{th}. Two different approaches were proposed for fatigue limit determination. In the first case, a stress level is applied in order to obtain some failures during the hold, which then allow the 'interrupted' strength distribution to be determined. The stress intensity factor corresponding to the weakest sample that survives the hold is calculated as the estimate for K_{th}, and this value is then determined as a function of increased hold time. In the second approach, sample sets are subjected to various stress levels. The stress intensity factor corresponding to 50% of failures occurring during the stress hold is assumed as the estimate K_{th}. The value of K_{th} is than re-determined as a function of hold time until it becomes invariant. The two approaches outlined above were considered to be preferable for materials with lower and higher Weibull moduli, respectively.

References

1. Stuart, D. A. & Anderson, O. L., Dependence of ultimate strength of glass under constant load on temperature, ambient atmosphere and time. *J. Am. Ceram. Soc.*, **36**(12) (1953) 416–24.
2. Shand, E. B., Experimental study of fracture of glass: I, The fracture process. *J. Am. Ceram. Soc.*, **37**(2) (1954) 52–60.
3. Mould, R. E. & Southwick, R. D., Strength and static fatigue of abraded glass under controlled ambient conditions: II, Effect of various abrasions and the universal fatigue curve. *J. Am. Ceram. Soc.*, **42**(12) (1959) 582–92.
4. Watanabe, M., Caporali, R. V. & Mould, R. E., The effect of chemical composition on the strength and static fatigue of soda-lime glass. *Phys. Chem. Glasses*, **2**(1) (1961) 12–23.
5. Mould, R. E., Strength and static fatigue of abraded glass under controlled ambient conditions: IV, Effect of surrounding medium. *J. Am. Ceram. Soc.*, **44**(10) (1961) 481–91.
6. Shand, E. B., Strength of glass — the Griffith method revised. *J. Am. Ceram. Soc.*, **48**(1) (1965) 43–9.
7. Hillig, W. B. & Charles, R. J., Surfaces, stresses-dependent surface reactions and strength. In *High Strength Materials*, ed. V. F. Zakay. John Wiley and Sons, New York, 1965, pp. 683–705.
8. Wiederhorn, S. M. & Bolz, L. H., Stress corrosion and static fatigue of glass. *J. Am. Ceram. Soc.*, **53**(10) (1970) 543–8.
9. Ritter, J. E. & Sherburne, C. L., Dynamic and static fatigue of silicate glasses. *J. Am. Ceram. Soc.*, **54**(12) (1971) 601–5.
10. Evans, A. G., A method for evaluating the time-dependent failure characteristics of brittle materials — and its application to polycrystalline alumina. *J. Mater. Sci.*, **7** (1972) 1137–46.
11. Evans, A. G., A simple method for evaluating slow crack growth in brittle materials. *Int. J. Fract.*, **9**(3) (1973) 267–75.
12. Wiederhorn, S. M. & Johnson, H., Effect of electrolyte pH on crack propagation in glass. *J. Am. Ceram. Soc.*, **56**(4) (1973) 192–7.
13. Wiederhorn, S. M., Subcritical crack growth in ceramics. In *Fracture Mechanics of Ceramics*, Vol. 2, eds. R. C. Bradt, D. P. H. Hasselman & F. F. Lange. Plenum Press, New York, 1974, pp. 613–46.
14. Wan, K., Lathabai, S. & Lawn, B. R., Crack velocity functions and threshold in brittle solids. *J. Eur. Ceram. Soc.*, **6** (1990) 259–68.
15. Chan, K. S. & Page, R. A., Origin of the creep-crack growth threshold in a glass-ceramic. *J. Am. Ceram. Soc.*, **75**(3) (1992) 603–12.
16. Pavelchek, E. K. & Doremus, R. H., Static fatigue in glass — a reappraisal. *J. Non-Cryst. Solids*, **20** (1976) 305–21.
17. Gehrke, E., Ullner, C. & Hähnert, M., Correlation between multistage crack growth and time-dependent strength in commercial silicate glasses. Part 1. Influence of ambient media and types of initial cracks. *Glastech. Ber.*, **60**(8) (1987) 268–78.
18. Gehrke, E., Ullner, C. & Hähnert, M., Correlation between multistage crack growth and time-dependent strength in commercial silicate glasses. Part 2. Influence of surface treatment. *Glastech. Ber.*, **60**(10) (1987) 340–5.
19. Gehrke, E., Ullner, C. & Hähnert, M., Effect of corrosive media on crack growth of model glasses and commercial silicate glasses. *Glastech. Ber.*, **63**(9) (1990) 255–65.
20. Fett, T., Germerdonk, K., Grossmüller, A., Keller, K. & Munz, D., Subcritical crack growth and threshold in borosilicate glass. *J. Mater. Sci.*, **26** (1991) 253–7.
21. Gehrke, E., Ullner, C. & Hähnert, M., Fatigue limit and crack arrest in alkali-containing silicate glasses. *J. Mater. Sci.*, **26** (1991) 5445–55.
22. Michalske, T. A., The stress corrosion limit: its measurement and implications. In *Fracture Mechanics of Ceramics*, Vol. 5, eds R. C. Bradt, D. P. H. Hasselman & F. F. Lange. Plenum Press, New York, 1983, pp. 277–89.
23. Dutton, R. & Rogowski, A. J., A theoretical study of crack propagation during high temperature static fatigue. *J. Can. Ceram. Soc.*, **41** (1972) 53–61.
24. Wilkins, B. J. S. & Dutton, R., Static fatigue limit with particular reference to glass. *J. Am. Ceram. Soc.*, **59**(3–4) (1975) 108–12.
25. Hayashi, K., Easler, T. E. & Bradt, R. C., A fracture statistics estimate of the fatigue limit of a borosilicate glass. *J. Eur. Ceram. Soc.*, **12** (1993) 487–91.
26. Minford, E. J. & Tressler, R. E., Determination of threshold stress intensity for crack growth at high temperature in silicon carbide ceramics. *J. Am. Ceram. Soc.*, **66**(5) (1983) 338–40.
27. Minford, E. J., Kupp, D. M. & Tressler, R. E., Static fatigue limit for sintered silicon carbide at elevated temperatures. *J. Am. Ceram. Soc.*, **66**(11) (1983) 769–73.
28. Foley, M. R. & Tressler, R. E., Threshold stress intensity for crack growth at elevated temperatures in a silicon nitride ceramic. *Adv. Ceram. Mater.*, **34** (1988) 383–6.
29. Yavuz, B. O. & Tressler, R. E., Threshold stress intensity for crack growth in silicon carbide ceramics. *J. Am. Ceram. Soc.*, **76**(4) (1993) 1017–24.
30. Tanaka, I. & Pezzotti, G., Evaluation of slow crack growth resistance in ceramics for high-temperature applications. *J. Am. Ceram. Soc.*, **75**(4) (1993) 772–7.

31. Evans, A. G. & Lange, F. F., Crack propagation and fracture in silicon carbide. *J. Mater. Sci.*, **10** (1975) 1659–64.
32. Jakus, K., Coyne, D. C. & Ritter, J. E., Analysis of fatigue data for lifetime predictions for ceramics materials. *J. Mater. Sci.*, **13** (1978) 2071–80.
33. DeSalvo, G. J., Theory and structural design application of Weibull statistics, Westinghouse Electric Corporation, Astronuclear Laboratory, Technical Report WANL-TME-2688, May 1970.
34. Ito, S. & Tomozawa, M., Crack blunting of high-silica glass. *J. Am. Ceram. Soc.*, **65**(8) (1982) 368–71.
35. Hirao, K. & Tomozawa, M., Dynamic fatigue of treated high-silica glass: explanation by crack tip blunting. *J. Am. Ceram. Soc.*, **70**(6) (1987) 377–82.
36. Hirao, K. & Tomozawa, M., Kinetics of crack tip blunting of glasses. *J. Am. Ceram. Soc.*, **71**(1) (1987) 43–8.
37. Han, W.-T. & Tomozawa, M., Mechanism of mechanical strength increase of soda-lime glass by aging. *J. Am. Ceram. Soc.*, **72**(10) (1989) 1837–43.